

MOL#41848

FUNCTIONAL CHARACTERIZATION OF A NUCLEOSIDE-DERIVED DRUG TRANSPORTER VARIANT (hCNT3C602R) SHOWING ALTERED SODIUM-BINDING CAPACITY

**Ekaitz Errasti-Murugarren, Pedro Cano-Soldado, Marçal Pastor-Anglada[†] and Fco Javier
Casado[†]**

**Departament de Bioquímica i Biologia Molecular, Facultat de Biologia, Universitat de
Barcelona, Spain.**

IBUB - Institut de Biomedicina de la Universitat de Barcelona, Spain

CIBER EHD, Spain

MOL#41848

Running title: hCNT3 polymorphism characterization

Address correspondence to: Fco Javier Casado, Departament de Bioquímica i Biologia
Molecular, Facultat de Biologia, Universitat de Barcelona, Avda Diagonal, 645 E-08028
Barcelona, Spain. Tel. 34 934034615; Fax. 34 934021559; E-mail: fcasado@ub.edu

Text pages: 25

Number of tables: 2

Number of figures: 6

Number of references: 34

Number of words in the Abstract: 229

Number of words in the Introduction: 472

Number of words in the Discussion: 1357

Abbreviations:

TMD: Transmembrane domain; **AZT:** Azidothymidine; **GFP:** Green fluorescent protein; **DMEM:** Dulbecco's modified eagle's medium; **WGA-TRITC:** Wheat germ agglutinin conjugated to tetramethylrhodamine isothiocyanate-dextran; **PFA:** Paraformaldehyde.

MOL#41848

Abstract

A novel cloned polymorphism of the human concentrative nucleoside transporter hCNT3 was described and functionally characterized. This variant consists of a T/C transition leading to the substitution of cysteine 602 by an arginine residue in the core of transmembrane domain 13. The resulting hCNT3_{C602R} protein has the same selectivity and affinity for natural nucleosides and nucleoside-derived drugs as hCNT3, but much lower concentrative capacity. The insertion of the transporter into a polarized membrane seems unaffected in the variant. In a preliminary survey of a typical Spanish population, this variant showed an allelic frequency of 1%. The functional impairment of the hCNT3_{C602R} polymorphism is attributable to the presence of an arginine rather than the loss of a cysteine at position 602, since an engineered hCNT3 protein with a serine residue at this position (hCNT3_{C602S}) and hCNT3 have similar kinetic parameters. The sodium activation kinetic analysis of both transporters revealed a variation in the affinity for sodium and a shift in the Hill coefficient, that could be consistent with a stoichiometry of 2:1 and 1:1 sodium:nucleoside, for hCNT3 and hCNT3_{C602R} respectively. In conclusion, the presence of an arginine residue in the core of TMD 13 is responsible for the different sodium affinity showed by the polymorphic transporter compared with the reference transporter. Individuals with the hCNT3_{C602R} variant might show a lower nucleoside and nucleoside analog concentrative capacity, which could be clinically relevant.

MOL#41848

Introduction

Nucleoside transporters mediate the uptake of both natural nucleosides and most nucleoside-derived antitumoral drugs (Pastor-Anglada et al., 2005; Pastor-Anglada et al., 1998). There are two families of nucleoside carriers in mammalian cells, the equilibrative ENT/SLC29A transporters, with low affinity and wide selectivity, and the concentrative CNT/SLC28A transporters, with higher affinity and more restricted selectivity (Baldwin et al., 1999; Griffith and Jarvis, 1996). Since absorptive cells in the renal and intestinal epithelia express all members of the concentrative CNT family (Errasti-Murugarren et al., 2007; Gutierrez and Giacomini, 1993; Ngo et al., 2001; Rodriguez-Mulero et al., 2005), any change in their activity might be highly relevant in the pharmacokinetics of nucleoside-derived drugs.

CNT3 is the least well characterized concentrative nucleoside transporter. It shows wide substrate selectivity, accepting both purine and pyrimidine nucleosides, and has a 2:1 Na^+ /nucleoside coupling ratio, allowing it to concentrate nucleosides intracellularly 10 times more efficiently than CNT1 or CNT2, which show a 1:1 Na^+ /nucleoside stoichiometry (Ritzel et al., 2001). Its role in drug transport is not well known, being involved in the uptake of cladribine and fludarabine (Mangravite et al., 2003) and cytosine arabinoside (Sarkar et al., 2005), as well as other non-nucleosidic drugs, such as the anthracycline pirarubicine (Nagai et al., 2005). Recently, CNT3 has also been shown to transport gemcitabine and the antiviral drugs AZT and ribavirin (Hu et al., 2006; Yamamoto et al., 2007). Its location at the apical membrane of a polarized cell model (Errasti-Murugarren et al., 2007; Mangravite et al., 2003) together with its presence along the rat and human renal tubule (Damaraju et al., 2007; Rodriguez-Mulero et al., 2005) and human intestine (Ritzel et al., 2001) suggest that CNT3 plays an important role in the absorption and disposition of nucleosides and synthetic nucleoside analogs.

Since CNT3 seems such an important element in the disposition of physiological nucleosides and nucleoside analogs, changes that affect its activity might have very relevant clinical repercussions. Heterogeneous patient response to treatment could be explained, at least in part, by inter-individual variability in the expression and/or activity of nucleoside transporters

MOL#41848

(Badagnani et al., 2005). An *ex vivo* analysis of nucleoside transporter activity and expression in chronic lymphocytic leukemia patients showed that variation in the transport rates of fludarabine correlated with its chemosensitivity, with CNT3 expression being the most variable among individuals (Molina-Arcas et al., 2003). Badagnani *et al.* identified up to 56 variable sites in the coding and flanking regions of the CNT3 gene, SLC28A3, in a survey of 270 DNA samples from different US populations (Badagnani et al., 2005). Ten of these coding variants resulted in amino acid changes and three of them had total allele frequencies higher than 1%. The functional characterization of these variants suggested that CNT3 tolerates very little non-synonymous change, at least in certain well-defined positions (Badagnani et al., 2005).

Here, we report a new polymorphism of the human SLC28A3 gene, a T/C transition that consists of an amino acid change in the hCNT3 protein sequence, with cysteine at position 602 being changed to an arginine. In consequence, the resulting hCNT3 protein shows altered sodium binding capacity, bearing similar affinities for its substrates but much lower concentrative capacity. This variant, which shows an allelic frequency of 1% in a typical Spanish population, sheds some new light on the molecular mechanisms underlying hCNT3 function.

MOL#41848

Materials and Methods

Plasmid Construction and Site-directed Mutagenesis – A normal portion of a kidney bearing a renal carcinoma and removed at surgery, according to the ethics review board of the IUNA (Institut d’Urologia, Nefrologia i Andrologia – Fundació Puigvert) was used to amplify a 2.2-kb human renal CNT3 (hCNT3) cDNA. Amplification was achieved using the primers 5’-CTAAATGAAGAGCGCTTGGGACCT-3’ and 5’-AGCATCTGTACTTCAGAGTTCCACTGG-3’, which corresponded to positions 1-24 and 2183-2209, respectively, of the published sequence with GenBank™ accession number AF305210, and cloned into pGEM vector (BD Biosciences, Clontech, Palo Alto, CA). This fragment was then subcloned into *KpnI* and *PstI* sites of the mammalian expression vector pcDNA3.1 (Invitrogen). Restriction sites were added using the following primers (restriction sites underlined): 5’-GGGGTACCGCATGGAGCTGAGGAG-3’ and 5’-AACTGCAGGGAGAAGAGGCTGACC-3’. To generate a GFP-tagged hCNT3 protein, the pEGFP-C1 (Clontech, Palo Alto, CA) and hCNT3-pcDNA3.1 plasmids were double-digested with *PstI* and *HindIII* and the hCNT3 insert was ligated into the pEGFP-C1 vector. The hCNT1 clone (GenBank™ accession number U62966) was obtained from human fetal liver (Mata et al., 2001). The cDNA was then subcloned into pcDNA3 and pEGFP-C1 vectors. The QuickChange™ site-directed mutagenesis kit (Stratagene, La Jolla, CA, USA) was used to convert codons for arginine 602 in cloned hCNT3 and serine 575 in hCNT1 to cysteine and arginine residues, respectively, according to the manufacturer's protocol. The pcDNA3.1- and GFP-fused hCNT3_{C602R} and hCNT1 constructs were used as templates. The R602C and C602S substitutions were introduced into hCNT3 using a compatible reverse primer and, as forward primers, 5’-CTGATTGCGGGGACCGTGGCCTGCTTCATGACAGCCTGCATCG-3’ or 5’-CTGATTGCGGGGACCGTGGCCAGCTTCATGACAGCCTGCATCG-3’, respectively. Both primers annealed to the coding sequence in the arginine 602 region, and the position of the codon for arginine 602, converted to a cysteine or to a serine residue respectively, was

MOL#41848

underlined. The S575R substitution was introduced into hCNT1 using as a forward primer 5'-CTTCACGGGAGCCTGTGTGCGCCTGGTGAACGCCTGTATGGC-3', which annealed to the coding sequence in the serine 575 region, and a compatible reverse primer. The position of the codon for serine 575 converted to an arginine residue was underlined. All constructions were verified by DNA sequencing in both directions and used for transient transfection.

Genotyping - Genomic DNA obtained from oral mucosa of 200 individuals with their informed consent, with a commercial kit (Qiagen, Hilden, Germany), was a generous gift from Dr. Dolors Colomer (Hospital Clínic, IDIBAPS, Barcelona, Spain). Genotyping was performed using allele-specific Taqman probes labeled with Vic and Fam. Primers and probes were designed by the manufacturer with Primer Express software (Taqman Assays-on-Demand, Applied Biosystems, Foster City, CA). Amplification reactions were performed in optical 384-well plates, using 20 ng of DNA. After amplification, fluorescence was read in an ABI7700 sequence detector (Applied Biosystems). The presence of this variant was verified by DNA sequencing.

Cell culture and transfection - Human cervix carcinoma HeLa cells and canine kidney epithelial cells (MDCK) were maintained at 37°C/5%CO₂ in DMEM (BioWhittaker) supplemented with 10% fetal bovine serum (v/v), 50 units/mL penicillin, 50 µg/mL streptomycin and 2mM L-glutamine. HeLa cells were transiently transfected with the plasmid constructions described above using Lipofectamine 2000 (Invitrogen, Carlsbad, CA, USA) and following the manufacturer's protocol. Nucleoside transport, confocal microscopy and flow cytometry analysis were carried out 24 hours after transfection.

MDCK cells were plated on transwell plates (Corning Costar, Cambridge, MA, USA; 3402; 12 mm diameter, 0.3 µm pore) and transfected as previously described (Harris et al., 2004).

Nucleoside and nucleobase transport assay - Uptake rates were measured as previously described (del Santo et al., 1998) by exposing replicate cultures at room temperature to the appropriate [³H]-labeled nucleoside or nucleobase (1 µM, 1µCi/mL, Moravsek Biochemicals or Amersham Pharmacia Biotech) in either a sodium-containing or a sodium-free transport buffer. Initial rates of transport were determined by an incubation of 1 min, and transport was

MOL#41848

terminated by washing in an excess of chilled buffer. Saturation kinetics were evaluated by non-linear regression analysis and the kinetic parameters derived from this method were confirmed by linear regression analysis. Sodium:nucleoside stoichiometry was calculated by measuring uridine uptake with varying concentrations of NaCl (0-100 mM) and then by analyzing the data with the Hill equation. Sodium concentrations were varied by combining the concentration of NaCl and choline chloride without changing the osmolality of the transport medium.

For inhibition kinetic studies cells were incubated with 1 μ M [3 H]-uridine (1 μ Ci/mL Amersham Pharmacia Biotech) and varying concentrations of unlabeled fludarabine (0-5000 μ M), 5-fluorouridine (0-5000 μ M) or cytarabine (0-10000 μ M). The Cheng-Prusoff equation was then used, when applicable, to calculate K_i values (Cheng and Prusoff, 1973), using calculated K_m values for uridine for the reference and polymorphic hCNT3 proteins (shown in Table 1).

Analysis of nucleoside transport and nucleoside vectorial flux on transwells - MDCK cells were grown on transwell filters, transfected and uptake rates monitored, as previously described (Harris et al., 2004). Filter inserts were washed three times in Na^+ or Na^+ -free buffer, and then 1 μ M [3 H]-uridine (Moravek Biochemicals) was added to the apical side. Transport experiments were conducted with buffer (0.5 mL in the apical compartment and 0.5 mL in the basal compartment) containing either sodium or choline on both sides of the Transwell filters. At various time points (up to 20 minutes), 50 μ L of buffer were collected from the basal compartment. The transport experiments were terminated by aspirating the buffer, and filters were washed in chilled buffer. The whole filter was wiped out with tissue to remove any excess buffer, removed from the plastic support and counted on a scintillation counter. The cells on the filters were solubilized by 0.1 % SDS and 100 mM NaOH.

Membrane insertion of hCNT3 and hCNT1 proteins - To determine whether the different hCNT3 and hCNT1 transporter variants were correctly inserted into the plasma membrane, confocal microscopy of GFP-fused chimeras was performed on a semi-confluent monolayer of transfected HeLa cells cultured on glass coverslips. Glass coverslip-grown cells were incubated with 1 μ g/mL WGA-TRITC for 30 min at 4°C, rinsed three times in phosphate-buffered saline- Ca^{2+} - Mg^{2+} , fixed for 15 min in PFA 3% sucrose 0.06M, rinsed three times in phosphate-

MOL#41848

buffered saline, and then mounted with aqua-poly/mount coverslipping medium (Polysciences, Inc. Warrington, PA). Images were obtained using an Olympus Fluoview 500 laser-scanning confocal microscope equipped with HeNe and Ar lasers as the light source. The colocalization of GFP-fused chimeras with plasma membrane WGA-TRITC was determined by quantifying the extent of pixel colocalization of GFP with TRITC fluorescence using Metamorph Imaging software (Universal Imaging, West Chester, PA), as described (Murph et al., 2003; Volpicelli et al., 2001). The background was subtracted from unprocessed images and the percentage of GFP pixels overlapping with TRITC pixels was measured. Data are presented as the mean \pm s.e.m. of measurements from 10 cells per sample. Transfection efficiency and fluorescence intensity per cell were determined by flow cytometry using a Cytomics FC 500 MPL Flow Cytometry System (Beckman Coulter).

To analyze the polarized membrane insertion of both hCNT3 proteins, 1.7×10^5 MDCK cells were grown in twelve-well Corning Costar polycarbonate Transwell filter inserts for 24 h and then transfected as explained previously. Cells were fixed as described above, then filters excised and loaded onto a glass slide and covered with a coverslip. Between the slide and the coverslip, a ~1-mm gap was filled with aqua-poly/mount coverslipping medium (Polysciences, Inc. Warrington, PA). Actin was stained using phalloidin-TRITC. Images were obtained as described above.

MOL#41848

Results

hCNT3 cDNA was amplified from a kidney sample. When sequenced, an unexpected change, a T/C transition at position 1804 (position relative to the ATG start site and based on the cDNA sequence) resulting in a non-conservative replacement of cysteine 602 by an arginine, was identified. This variation is located at TMD13 of the transporter protein. As shown in Figure 1, this cysteine is conserved among human, rat, mouse and hagfish orthologs. Thus, this variation affects a highly conserved cysteine residue in the core of the TMD13. Since this change might have functional implications, we decided, first, to study whether the T/C variation (C602R) of the cloned transporter corresponded to a variant present in a typical Spanish population. The genotype analysis showed this variant to be present in two chromosome of the 400 analyzed, thus yielding an allelic frequency of 1%, a value similar to that previously reported for other hCNT3 variants (Badagnani et al., 2005).

Secondly, we addressed whether this variant could affect the hCNT3-related function. To do so, we expressed the hCNT3_{C602R} variant as well as the reference counterpart (hCNT3), corresponding to the published sequence with GenBankTM accession number AF305210. Figure 2 shows the sodium-dependent uptake rates of a panel of natural nucleosides (uridine, cytidine, thymidine, guanosine and adenosine) and a nucleobase (hypoxanthine) measured in hCNT3- and hCNT3_{C602R}-transfected HeLa cells. Both isoforms had identical selectivity, similar to that described previously (Ritzel et al., 2001), although transport rates were significantly lower in the polymorphic than in the reference transporter. When cysteine 602 was mutated to a serine, the engineered protein showed the same selectivity and transport rates as those found for hCNT3 (data not shown), suggesting that the presence of arginine at position 602, rather than the lack of cysteine, was responsible for the lower transport rate shown by the hCNT3_{C602R} variant. Mutation of the equivalent residue in the other pyrimidine nucleoside-transporting isoform, hCNT1, completely blocked the transport of all the nucleosides assayed, even when used at much higher concentrations (Fig. 2B).

MOL#41848

Concentration-dependence curves for uridine, cytidine, thymidine, guanosine and adenosine uptake, measured as initial rates of transport (1 min), in hCNT3- and hCNT3_{C602R}-transfected HeLa cells were determined. The concentration-dependent uptake by both isoforms was saturable and conformed to Michaelis-Menten kinetics. Kinetic parameters, apparent K_m and V_{max} , were calculated by fitting the transport data to the Michaelis-Menten equation and the resulting values were confirmed by linear regression. The mean \pm s.e.m. values (n=3) for K_m and V_{max} for both transporters are shown in Table 1. Thus, in the case of the polymorphic variant, the apparent K_m for all the assayed natural nucleosides was identical to that observed for hCNT3, but V_{max} was nearly 4-fold lower than that found for the reference transporter. Kinetic parameters of hCNT3_{C602S} were not significantly different from those obtained for hCNT3 (not shown).

We next investigated whether the reduced activity of the hCNT3_{C602R} and the null activity of the mutated hCNT1 were due to impaired insertion into the membrane. Transiently transfected HeLa cells expressing GFP- fused chimeras of hCNT3, hCNT3_{C602R}, hCNT1 or hCNT1_{S575R} were incubated with the plasma membrane marker WGA-TRITC for 30 min at 4°C to avoid Golgi staining. All the constructions showed a similar sub-cellular pattern (Fig. 3), being located predominantly at the plasma membrane and, to a lesser extent, at the Golgi complex, which may represent a newly synthesized transporter en route to the plasma membrane. To quantify GFP-fused transporter membrane insertion, we measured colocalization with the plasma membrane WGA-TRITC, using Metamorph image analysis (Murph et al., 2003; Volpicelli et al., 2001). All the constructions showed similar colocalization percentages (Table 2), and flow cytometry showed the same transfection rate and fluorescence intensity for both pairs of transporters (hCNT3 vs hCNT3_{C602R} and hCNT1 vs hCNT1_{S575R}). Taken together, these results indicate that insertion into the membrane was unaltered in both engineered transporters.

To determine whether this hCNT3 variant could show altered sodium binding capacity, the initial rate of sodium-dependent uridine uptake (1 μ M) was determined as a function of extracellular sodium concentration (0-100 mM) in HeLa cells transfected with cDNA encoding

MOL#41848

either hCNT3 or hCNT3_{C602R}. Figure 4 shows that the relationship for hCNT3 between uridine influx and extracellular sodium concentration was sigmoidal, while the sodium-dependent uridine uptake mediated by the hCNT3_{C602R} was hyperbolic. Hill coefficients derived from these data were 2.2 ± 0.17 and 0.74 ± 0.2 for hCNT3 and its variant, respectively, whereas K_{50} for Na⁺ were 18.04 ± 1.38 mM and 3.38 ± 1.02 mM, respectively. These results would suggest a sodium:nucleoside stoichiometry for hCNT3 of 2:1 whereas the hCNT3 variant would display a 1:1 coupling ratio.

Since hCNT3 is an apically located transporter in epithelia and its expression is known to determine nucleoside vectorial flux (Errasti-Murugarren et al., 2007) we proceeded to determine, first, whether the variant could be inserted in the same way into the membrane in a polarized manner and, secondly, whether this would affect vectorial flux of nucleosides across the epithelial barrier. Transfection of cDNA encoding GFP-fused transporter constructs showed, that both hCNT3 and hCNT3_{C602R} were inserted at the apical membrane of polarized MDCK cells grown in a transwell dish (not shown), thus indicating that polymorphism did not affect proper insertion into a polarized membrane. Due to the important role of the hCNT3 in the transepithelial flux of nucleosides (Errasti-Murugarren et al., 2007), the vectorial flux of uridine was studied by using MDCK cells transfected with cDNA encoding either hCNT3 or hCNT3_{C602R} or empty pcDNA3.1 vector, to analyze the effect of the variation on the net uridine flux across the epithelial barrier. Figure 5 shows the sodium-dependent transepithelial flux of uridine (A) and the intracellular accumulation (B) in hCNT3-, hCNT3_{C602R}- and mock-MDCK cells. As expected, both vectorial flux and intracellular accumulation were significantly lower in epithelia expressing the polymorphic variant than in cells expressing the reference hCNT3. Nevertheless, a net sodium-dependent transepithelial flux and accumulation of uridine were still established in the presence of this variant.

We also examined the functional consequences of the variant using the antileukemic analogs fludarabine and cytarabine and the antineoplastic drug 5-fluorouridine. Figure 6 shows the uptake of 1 μ M [³H]-uridine in the presence of increasing concentrations of fludarabine (upper), 5-fluorouridine (middle) or cytarabine (lower) measured in hCNT3 and hCNT3_{C602R}

MOL#41848

expressing HeLa cell line. The K_i values revealed no differences in the interaction affinity of the assayed nucleoside analogs for both hCNT3 and the polymorphic variant.

MOL#41848

Discussion

CNT3 plays an important role in the uptake and bioavailability of both natural and modified nucleosides due to its broad substrate selectivity and sodium:nucleoside stoichiometry (2:1 for CNT3 compared to 1:1 for CNT1 and CNT2), which allows concentrating its substrates 10-fold higher than the rest of the concentrative nucleoside transporters (Ritzel et al., 2001). Due to the capital role of CNT3 in maintaining the homeostasis of endogenous nucleosides, sequence variations affecting transporter activity could be relevant, not only because they might provide new insights into the structure-function relationship of the transporter protein, but also because these variants might have patho-physiological implications.

Human CNT3 cDNA is 2210 bp long (GenBankTM accession number AF305210) and encodes a protein of 691 amino acids. At the level of amino acid sequence, human CNT3 is 77% identical to rat CNT3, 78% identical to mouse CNT3 and 57% identical to hagfish CNT. Residues within TMDs 4-13 are particularly highly conserved among hCNT3 and other orthologs, suggesting that these regions contain the functional core of the proteins. The C602R variant identified herein results in a radical chemical change, with a Grantham value of 180 (Grantham, 1974), and is found at the core of TMD 13. This transmembrane domain may play a crucial role in transporter activity, as suggested by our results. When this variation was introduced into the hCNT1 transporter (hCNT1_{S575R}), an hCNT3 paralog, the resulting mutated transporter failed to transport any of the assayed substrates, which further supports the view that this TM domain is also important for hCNT1 function and is consistent with previous structure-function data, suggesting that these TMDs are relevant for substrate recognition and translocation (Zhang et al., 2006).

Since this variant was identified by serendipity, we were interested in assessing its occurrence in humans. A preliminary genomic analysis in a typical Spanish population revealed a T/C transition at position 1804 (leading to a non-conservative C602R substitution), a hitherto unreported polymorphic variant. It was detected in two chromosome of the 400 analyzed, thus yielding an allelic frequency for the C602R variant of 1%, similar to that previously described

MOL#41848

by Bagdanani *et al.* for some non-synonymous hCNT3 variants. This variant was not identified in any of the previous studies on hCNT3 sequence analysis (Badagnani et al., 2005; Damaraju et al., 2005) suggesting a population specific incidence, as observed for other variants. The C602R change affected an evolutionarily conserved residue, which is also conserved in its orthologs in equivalent positions. The variant C602R has a reduced functional transport capability for both purine and pyrimidine nucleosides, although the affinity for both natural and derived nucleosides was identical in both transporters. It also resulted in a reduced transepithelial flux when transfected into a polarized model (MDCK) compared to reference transporter, as well as in a reduced intracellular accumulation. These observations are consistent with findings that hCNT3 is under strong negative selection, as deduced from the few non-synonymous variants it presents, most of which are singletons (Badagnani et al., 2005) and because changes at evolutionarily conserved residues are most likely to be deleterious to protein function (Leabman et al., 2003; Miller and Kumar, 2001). Due to its broad selectivity and high concentrative capacity and its presence in absorptive epithelia like intestine (Ritzel et al., 2001) and renal tubules (Damaraju et al., 2007; Rodriguez-Mulero et al., 2005), CNT3 could play a pivotal role in nucleoside homeostasis and in the pharmacokinetics of nucleoside-derived drugs.

The expression of this transporter variant may result in reduced intestinal absorption as well as defective renal re-absorption of nucleosides, both natural and synthetic, which are effectively transported by CNT3. However, the possibility that the other two CNT proteins would compensate for a decreased efficiency of CNT3 function cannot be ruled out but could not be tested because we genotyped a blind genomic DNA biobank.

Biochemical evidence was provided showing that the decreased V_{max} of the hCNT3 variant was the result of altered sodium binding capacity, since expression at the plasma membrane was unaffected. The polymorphic variant was also inserted into the proper membrane compartment when studied in a polarized epithelial cell line such as MDCK, showing an apical localization as described previously (Mangravite et al., 2003). The sodium dependence analysis of uridine uptake revealed a sigmoidal kinetics for hCNT3, whereas this relationship was hyperbolic for hCNT3_{C602R}. The Hill coefficient for hCNT3 was similar to those previously

MOL#41848

described (close to 2) (Ritzel et al., 2001; Toan et al., 2003), thus consistent with a 2:1 sodium:nucleoside stoichiometry. However, this coefficient for hCNT3_{C602R} and the K_m for sodium pointed towards a shift from a 2:1 to a 1:1 sodium:nucleoside concentrative nucleoside transporter, similar to the behaviour of hCNT1 for which a 1:1 stoichiometry has been reported (23). Thus, the lower concentrative ability of the polymorphic C602R variant compared to the hCNT3 could be due to its conversion into a 1:1 sodium:nucleoside transporter, which in principle should be 10-fold less concentrative than a 2:1 carrier. However, another possible explanation was that this variant could be affecting V_{max} for reasons other than a change in stoichiometry. Maybe with an increased affinity for sodium, a transport cycle takes longer as it takes a longer time for the sodium to dissociate from the binding site. At steady state, uptake is determined by the balance between influx and leak back out of the cell. If influx is decreased and leak is unchanged, then net steady state uptake will be decreased. Smith *et al.* showed that hCNT3 is functionally active in the presence of a proton gradient across the plasma membrane with a proton:nucleoside stoichiometry of 1:1 and it seems that both sodium and proton binding sites are located in the same region of hCNT3. Their results suggest that hCNT3 might translocate substrates in a 1:1 sodium:nucleoside coupling ratio and such a possibility is also suggested here by analysis of this novel variant of hCNT3. Thus, these results could be consistent with a sequential mechanism of transport in which sodium binds to the transporter first, increasing its affinity for the nucleoside, which then binds to the transporter (Jauch and Lauger, 1986; Klamo et al., 1996; Mackenzie et al., 1996). They also suggest that the second sodium ion that binds CNT3 is involved in increasing the concentrative ability of the transporter by enhancing its V_{max} .

Taking all our results together, it seems that the presence of arginine residue in the core of TMD13 would be responsible for the altered sodium binding capacity of the hCNT3_{C602R} variant. When the cysteine at position 602 was mutated into a serine, kinetic parameters of this hCNT3_{C602S}-engineered protein were similar to those obtained for hCNT3, thus suggesting that the feature responsible for low activity was the presence of the arginine residue rather than the lack of the cysteine residue at position 602. This observation suggested that it was the presence

MOL#41848

of a positive charge (arginine at physiological pH is protonated) inside the TMD13 helix rather than the lack of cysteine that caused the reduced activity, either due to an electrostatic effect or to structure changes, or both. The lack of a crystal structure for hCNT3 or any other CNT protein makes it difficult to advance further in this hypothesis. Yamashita *et al.* (Yamashita et al., 2005), working with the bacterial homologue of the mammalian Na⁺/Cl⁻ neurotransmitter transporter, described the presence of two separate sodium-binding sites, each formed by several amino acids from various TM domains that spatially comprised a sodium-binding pocket. Considering a similar model for hCNT3, a positive charge near one of the two sodium-binding sites could result in electrostatic repulsion between the sodium ion and the arginine residue. Alternatively, the presence of arginine at position 602 could compromise the TMD13 structure, affecting one of the sodium binding sites and thus preventing sodium-binding to it. These data were consistent with a recent finding (Zhang et al., 2006) that suggests an important structural role for this TM segment as well as a possible role in the recognition of substrates. The possibility that TMD13 is, at least in part, involved in sodium recognition is also consistent with recent data suggesting that structural determinants of sodium/nucleoside stoichiometry reside in the C-terminal half of the protein (Smith et al., 2005).

In summary, the present study reports the existence of a polymorphic variant of the human concentrative nucleoside transporter CNT3 (the C602R substitution) that severely affects its functionality and that could be of physiological and pharmacological relevance. A single substitution in TMD13 results in reduced V_{max} and impaired vectorial flux and accumulation of nucleosides across epithelia. This variant also highlights the important role that TMD13 might play in sodium binding and translocation. Further genotyping of human populations is required to figure out to what extent this variant is abundant in different ethnic groups or in patients with particular diseases.

Acknowledgements

We would like to thank Dr. Dolors Colomer (Hospital Clínic, Barcelona) for access to DNA samples and Dr. José Ballarín (IUNA) for access to a kidney sample.

MOL#41848

References

- Badagnani I, Chan W, Castro RA, Brett CM, Huang CC, Stryke D, Kawamoto M, Johns SJ, Ferrin TE, Carlson EJ, Burchard EG and Giacomini KM (2005) Functional analysis of genetic variants in the human concentrative nucleoside transporter 3 (CNT3; SLC28A3). *Pharmacogenomics J* **5**:157-165.
- Baldwin SA, Mackey JR, Cass CE and Young JD (1999) Nucleoside transporters: molecular biology and implications for therapeutic development. *Mol Med Today* **5**:216-24.
- Cheng Y and Prusoff WH (1973) Relationship between the inhibition constant (K_i) and the concentration of inhibitor which causes 50 per cent inhibition (I₅₀) of an enzymatic reaction. *Biochem Pharmacol* **22**:3099-3108.
- Damaraju S, Zhang J, Visser F, Tackaberry T, Dufour J, Smith KM, Slugoski M, Ritzel MW, Baldwin SA, Young JD and Cass CE (2005) Identification and functional characterization of variants in human concentrative nucleoside transporter 3, hCNT3 (SLC28A3), arising from single nucleotide polymorphisms in coding regions of the hCNT3 gene. *Pharmacogenet Genomics* **15**:173-182.
- Damaraju VL, Elwi AN, Hunter C, Carpenter P, Santos C, Barron GM, Sun X, Baldwin SA, Young JD, Mackey JR, Sawyer MB and Cass CE (2007) Localization of broadly selective equilibrative and concentrative nucleoside transporters, hENT1 and hCNT3, in human kidney. *Am J Physiol Renal Physiol* **293**:F200-211.
- del Santo B, Valdes R, Mata J, Felipe A, Casado FJ and Pastor-Anglada M (1998) Differential expression and regulation of nucleoside transport systems in rat liver parenchymal and hepatoma cells. *Hepatology* **28**:1504-1511.
- Errasti-Murugarren E, Pastor-Anglada M and Casado FJ (2007) Role Of Cnt3 In The Transepithelial Flux Of Nucleosides And Nucleoside-Derived Drugs. *J Physiol*.
- Grantham R (1974) Amino acid difference formula to help explain protein evolution. *Science* **185**:862-864.
- Griffith DA and Jarvis SM (1996) Nucleoside and nucleobase transport systems of mammalian cells. *Biochim Biophys Acta* **1286**:153-181.
- Gutierrez MM and Giacomini KM (1993) Substrate selectivity, potential sensitivity and stoichiometry of Na(+)-nucleoside transport in brush border membrane vesicles from human kidney. *Biochim Biophys Acta* **1149**:202-208.
- Harris MJ, Kagawa T, Dawson PA and Arias IM (2004) Taurocholate transport by hepatic and intestinal bile acid transporters is independent of FIC1 overexpression in Madin-Darby canine kidney cells. *J Gastroenterol Hepatol* **19**:819-825.
- Hu H, Endres CJ, Chang C, Umapathy NS, Lee EW, Fei YJ, Itagaki S, Swaan PW, Ganapathy V and Unadkat JD (2006) Electrophysiological characterization and modeling of the structure activity relationship of the human concentrative nucleoside transporter 3 (hCNT3). *Mol Pharmacol* **69**:1542-1553.
- Jauch P and Lauger P (1986) Electrogenic properties of the sodium-alanine cotransporter in pancreatic acinar cells: II. Comparison with transport models. *J Membr Biol* **94**:117-27.
- Klamo EM, Drew ME, Landfear SM and Kavanaugh MP (1996) Kinetics and stoichiometry of a proton/myo-inositol cotransporter. *J Biol Chem* **271**:14937-14943.
- Leabman MK, Huang CC, DeYoung J, Carlson EJ, Taylor TR, de la Cruz M, Johns SJ, Stryke D, Kawamoto M, Urban TJ, Kroetz DL, Ferrin TE, Clark AG, Risch N, Herskowitz I and Giacomini KM (2003) Natural variation in human membrane transporter genes reveals evolutionary and functional constraints. *Proc Natl Acad Sci U S A* **100**:5896-5901.
- Mackenzie B, Loo DD, Panayotova-Heiermann M and Wright EM (1996) Biophysical characteristics of the pig kidney Na⁺/glucose cotransporter SGLT2 reveal a common mechanism for SGLT1 and SGLT2. *J Biol Chem* **271**:32678-32683.

MOL#41848

- Mangravite LM, Badagnani I and Giacomini KM (2003) Nucleoside transporters in the disposition and targeting of nucleoside analogs in the kidney. *Eur J Pharmacol* **479**:269-281.
- Mata JF, Garcia-Manteiga JM, Lostao MP, Fernandez-Veledo S, Guillen-Gomez E, Larrayoz IM, Lloberas J, Casado FJ and Pastor-Anglada M (2001) Role of the human concentrative nucleoside transporter (hCNT1) in the cytotoxic action of 5[Prime]-deoxy-5-fluorouridine, an active intermediate metabolite of capecitabine, a novel oral anticancer drug. *Mol Pharmacol* **59**:1542-1548.
- Miller MP and Kumar S (2001) Understanding human disease mutations through the use of interspecific genetic variation. *Hum Mol Genet* **10**:2319-2328.
- Molina-Arcas M, Bellosillo B, Casado FJ, Montserrat E, Gil J, Colomer D and Pastor-Anglada M (2003) Fludarabine uptake mechanisms in B-cell chronic lymphocytic leukemia. *Blood* **101**:2328-2334.
- Murph MM, Scaccia LA, Volpicelli LA and Radhakrishna H (2003) Agonist-induced endocytosis of lysophosphatidic acid-coupled LPA1/EDG-2 receptors via a dynamin2- and Rab5-dependent pathway. *J Cell Sci* **116**:1969-1980.
- Nagai K, Nagasawa K and Fujimoto S (2005) Uptake of the anthracycline pirarubicin into mouse M5076 ovarian sarcoma cells via a sodium-dependent nucleoside transport system. *Cancer Chemother Pharmacol* **55**:222-230.
- Ngo LY, Patil SD and Unadkat JD (2001) Ontogenic and longitudinal activity of Na(+)-nucleoside transporters in the human intestine. *Am J Physiol Gastrointest Liver Physiol* **280**:G475-481.
- Pastor-Anglada M, Cano-Soldado P, Molina-Arcas M, Lostao MP, Larrayoz I, Martinez-Picado J and Casado FJ (2005) Cell entry and export of nucleoside analogues. *Virus Res* **107**:151-164.
- Pastor-Anglada M, Felipe A and Casado FJ (1998) Transport and mode of action of nucleoside derivatives used in chemical and antiviral therapies. *Trends Pharmacol Sci* **19**:424-430.
- Ritzel MW, Ng AM, Yao SY, Graham K, Loewen SK, Smith KM, Ritzel RG, Mowles DA, Carpenter P, Chen XZ, Karpinski E, Hyde RJ, Baldwin SA, Cass CE and Young JD (2001) Molecular identification and characterization of novel human and mouse concentrative Na⁺-nucleoside cotransporter proteins (hCNT3 and mCNT3) broadly selective for purine and pyrimidine nucleosides (system cib). *J Biol Chem* **276**:2914-2927.
- Rodriguez-Mulero S, Errasti-Murugarren E, Ballarin J, Felipe A, Doucet A, Casado FJ and Pastor-Anglada M (2005) Expression of concentrative nucleoside transporters SLC28 (CNT1, CNT2, and CNT3) along the rat nephron: effect of diabetes. *Kidney Int* **68**:665-672.
- Sarkar M, Han T, Damaraju V, Carpenter P, Cass CE and Agarwal RP (2005) Cytosine arabinoside affects multiple cellular factors and induces drug resistance in human lymphoid cells. *Biochem Pharmacol* **70**:426-432.
- Smith KM, Slugoski MD, Loewen SK, Ng AM, Yao SY, Chen XZ, Karpinski E, Cass CE, Baldwin SA and Young JD (2005) The broadly selective human Na⁺/nucleoside cotransporter (hCNT3) exhibits novel cation-coupled nucleoside transport characteristics. *J Biol Chem* **280**:25436-25449.
- Toan SV, To KK, Leung GP, de Souza MO, Ward JL and Tse CM (2003) Genomic organization and functional characterization of the human concentrative nucleoside transporter-3 isoform (hCNT3) expressed in mammalian cells. *Pflugers Arch* **447**:195-204.
- Volpicelli LA, Lah JJ and Levey AI (2001) Rab5-dependent trafficking of the m4 muscarinic acetylcholine receptor to the plasma membrane, early endosomes, and multivesicular bodies. *J Biol Chem* **276**:47590-47598.
- Yamamoto T, Kuniki K, Takekuma Y, Hirano T, Iseki K and Sugawara M (2007) Ribavirin uptake by cultured human choriocarcinoma (BeWo) cells and *Xenopus laevis* oocytes expressing recombinant plasma membrane human nucleoside transporters. *Eur J Pharmacol* **557**:1-8.

MOL#41848

- Yamashita A, Singh SK, Kawate T, Jin Y and Gouaux E (2005) Crystal structure of a bacterial homologue of Na⁺/Cl⁻-dependent neurotransmitter transporters. *Nature* **437**:215-223.
- Zhang J, Tackaberry T, Ritzel MW, Raborn T, Barron G, Baldwin SA, Young JD and Cass CE (2006) Cysteine-accessibility analysis of transmembrane domains 11-13 of human concentrative nucleoside transporter 3. *Biochem J* **394**:389-398.

MOL#41848

Footnotes

This work has been supported by grants PI-020934 from Fondo de Investigaciones Sanitarias, Ministerio de Sanidad y Consumo, BFU2006-07556/BFI, and Fundación Ramón Areces to F. Javier Casado and SAF2005-01259 from Dirección General de Ciencia y Tecnología, Ministerio de Educación y Ciencia, and FIPSE to Marçal Pastor-Anglada, and 2005SGR00315 from Direcció General de Recerca, DURSI, Generalitat de Catalunya, to Marçal Pastor-Anglada. Ekaitz Errasti-Murugarren and Pedro Cano-Soldado were recipient of FPU and FPI fellowships, respectively, from Ministerio de Educación y Ciencia. [†] These two authors contributed equally to the article

Reprints Request:

Fco Javier Casado

Departament de Bioquímica i Biologia Molecular

Facultat de Biologia. Universitat de Barcelona,

Avda Diagonal, 645 E-08028 Barcelona, Spain.

Tel. 34 934034615; Fax. 34 934021559

e-mail: fcasado@ub.edu

MOL#41848

Figure legends

Fig. 1. Primary structure of human CNT3 transmembrane domain 13. The aminoacid sequence of human TMD13 of CNT3 (hCNT3, GenBankTM accession number AF305210) is compared with that of hagfish CNT (hfCNT, GenBankTM accession number AF132298), rat (rCNT3, GenBankTM accession number AY059414), mouse (mCNT3, GenBankTM accession number AF305211) and polymorphic transporter (hCNT3_{C602R}). The regions of sequence conservation between proteins are boxed.

Fig. 2. Sodium-dependent uptake of [³H]-labeled nucleosides and nucleobase by recombinant nucleoside transporters expressed in HeLa cell line. Uptake of nucleoside and nucleobase (1 μM, 1 min) by hCNT3 (close bars) or hCNT3_{C602R} (open bars) (A) and hCNT1 (close bars) or hCNT1_{S575R} (open bars) (B) was measured in transport medium containing 137 mM NaCl or 137 mM choline chloride. Sodium-dependent transport was calculated as uptake in NaCl medium minus uptake in choline chloride. Data are expressed as the mean ± s.e.m. of three experiments carried out on different days on different batches of cells.

Fig. 3. Subcellular localization of GFP-fused chimeras. HeLa cells were transiently transfected with pEGFPC1-fused hCNT3 or hCNT3_{C602R} (A) or pEGFPC1-hCNT1 or hCNT1_{S575R} (B) and were incubated with 1 μg/ml WGA-TRITC for 30 minutes at 4°C. The cells were fixed and processed for fluorescence localization of the transfected transporters.

Fig. 4. Sodium dependence of influx of uridine mediated by recombinant hCNT3 and hCNT3_{C602R}. Transporter-mediated uptake of [³H]-uridine (1 μM, 1 min) by hCNT3 (A) and hCNT3_{C602R} (B) was measured in transport medium containing 0-100 mM NaCl using choline chloride to maintain isosmolality. Mediated transport was calculated as uptake in transporter transfected cells minus mock transfected cells in which uridine uptake is not sodium-dependent. *Inset:* Hill plots of hCNT3 and hCNT3_{C602R} data, respectively. *K_m* values and Hill coefficients

MOL#41848

(*n*) are 18.04 ± 1.38 mM and 2.2 ± 0.17 respectively for hCNT3 and 3.38 ± 1.02 mM and 0.74 ± 0.2 for the polymorphic transporter. Data are expressed as the mean \pm s.e.m. of three experiments carried out on different days on different batches of cells.

Fig. 5. Transepithelial flux of uridine in MDCK cells transfected with cDNA encoding either hCNT3 or hCNT3_{C602R} or empty pcDNA3.1. (A) Sodium-dependent transepithelial flux of [³H]-uridine (1 μM) in MDCK cells transfected with cDNA encoding either hCNT3 (■), or polymorphic transporter (▲) or empty pcDNA3.1 (▼) from the apical to the basolateral compartment. (B) Sodium-dependent intracellular accumulation of uridine measured in hCNT3- (open bar), hCNT3_{C602R}- (close bar) and mock- (striped bar) transfected MDCK-cells after 20 minutes. Data are expressed as the mean \pm s.e.m. of uptake values obtained in three wells or filter inserts. Data are representative of three experiments carried out on different days on different batches of cells.

Fig. 6. Kinetics of inhibition of [³H]-uridine uptake by nucleoside-derived drugs in HeLa cells transfected with cDNA encoding either hCNT3 or hCNT3_{C602R}. Transporter-mediated uptake of [³H]-uridine (1 μM, 1 min) by hCNT3 (■) and hCNT3_{C602R} (▲) was inhibited with varying concentrations of fludarabine (upper), 5-fluorouridine (middle) or cytarabine (lower). To determine *K_i* values, data were fit to non-linear regression using *GraphPad Prism* software. *K_i* values for hCNT3 and hCNT3_{C602R} were 344.47 μM and 335.98 μM respectively for fludarabine, 5.66 μM and 6.45 μM respectively for 5-fluorouridine and 16.23 mM and 13.43 mM respectively for cytarabine. Data are expressed as the mean \pm s.e.m. of three experiments carried out on different days on different batches of cells.

MOL#41848

Table 1. Apparent K_m and V_{max} for [3 H]-nucleoside uptake by hCNT3 and hCNT3_{C602R} transiently expressed in HeLa cells.

Nucleosides	hCNT3		hCNT3 _{C602R}	
	K_m (μ M)	V_{max} (pmol/mg/min)	K_m (μ M)	V_{max} (pmol/mg/min)
Uridine	5.3 \pm 1.2	484.6 \pm 15.6	5.9 \pm 1.5	140.8 \pm 12.6
Cytidine	3.5 \pm 0.4	401.7 \pm 30.8	3.9 \pm 0.9	112.6 \pm 11.6
Thymidine	10.6 \pm 2.2	645.2 \pm 29.6	9.5 \pm 2.9	186.7 \pm 15.8
Adenosine	2.4 \pm 1.1	579.2 \pm 34.5	2.2 \pm 0.8	160.6 \pm 12.7
Guanosine	8.5 \pm 2.2	458.5 \pm 33.4	9.1 \pm 1.5	131.5 \pm 12.5

Table 1. Kinetic parameters K_m and V_{max} for hCNT3 and hCNT3_{C602R} in HeLa transient transfectants. Transport assays with hCNT3 and hCNT3_{C602R} HeLa transfectants were performed with graded concentrations of [3 H]-labeled nucleosides in sodium-containing and sodium-free transport buffer as described under *Materials and Methods*. The sodium-dependent component of [3 H]-labeled nucleosides uptake rates were plotted as a function of the nucleoside concentration tested (0-1000 μ M). Results are the mean of triplicate determinations. The data were analyzed by nonlinear regression using *GraphPad Prism* software. Data are expressed as the mean \pm s.e.m. of three experiments carried out on different days on different batches of cells.

MOL#41848

Table 2. Transfection efficiency, fluorescence intensity, and colocalization percentage in HeLa cells transfected with cDNA encoding GFP-fused chimeras with WGA-TRITC.

Construction	Transfection %	SEM	Fluorescence Intensity (a.u.)	SEM	Colocalization %	SEM
hCNT3	77.87	2.01	236.6	8.89	82.59	1.09
hCNT3 _{C602R}	78	1.71	241.47	6.44	80.12	1.54
hCNT1	80.6	1.14	208.5	1.73	77.63	2.64
hCNT1 _{S575R}	78.65	1.88	202.63	3.4	77.84	2.97

Table 2. Transfection efficiency, fluorescence intensity and colocalization percentage of GFP-fused chimeras with WGA-TRITC. HeLa cells were transfected with the cDNA encoding GFP-fused chimeras and after 24 hours cells were fixed and processed for fluorescence localization. The extent of colocalization between nucleoside transporters and WGA-TRITC was quantified using *Metamorph* image analysis as described in *Materials and Methods*. On the other hand transfected cells were resuspended and analyzed by flow cytometry for transfection efficiency and construction expression rate. Data are expressed as the mean \pm s.e.m. of three experiments carried out on different days on different batches of cells.

hfCNT3	IRALIAGTACFSTACIAGVI
rcCNT3	MRALIAGTACFMTACIAGMI
mcCNT3	MRALIAGTACFMTACIAGII
hCNT3	VRALIAGTVACFMTACIAGII
hCNT3C602R	VRALIAGTVAREFMTACIAGII

Figure 1

Figure 2

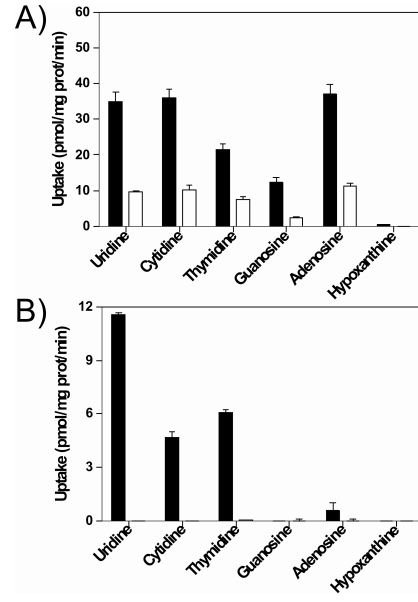


Figure 3

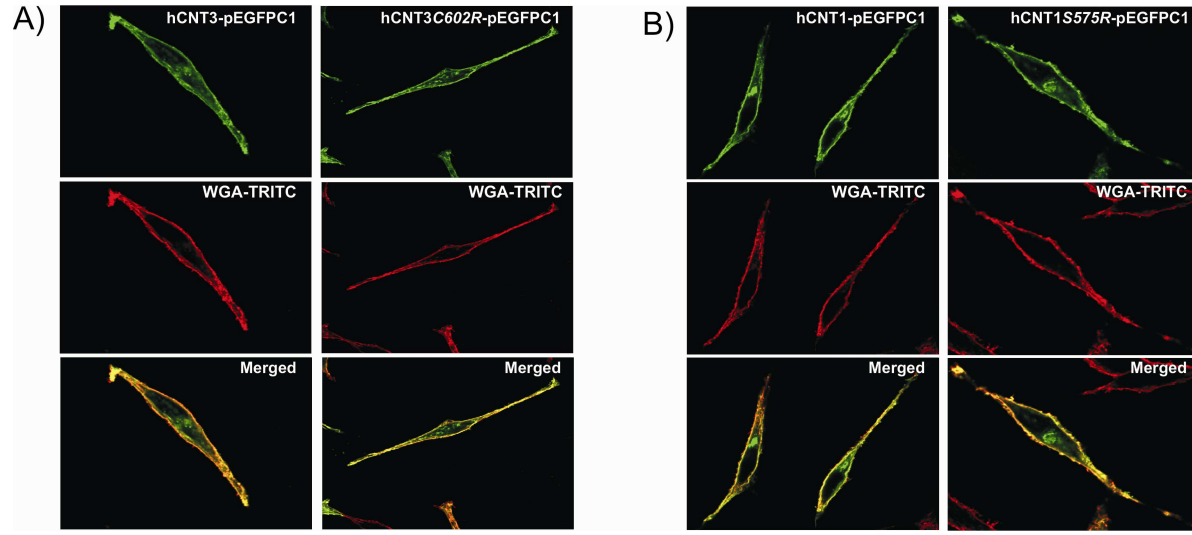


Figure 4

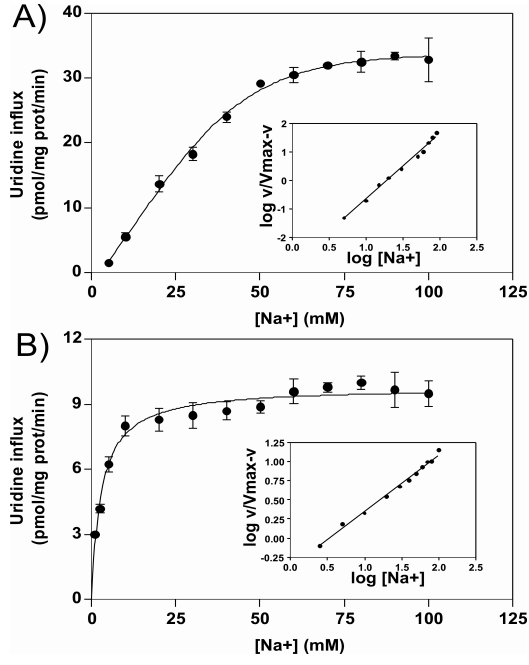


Figure 5

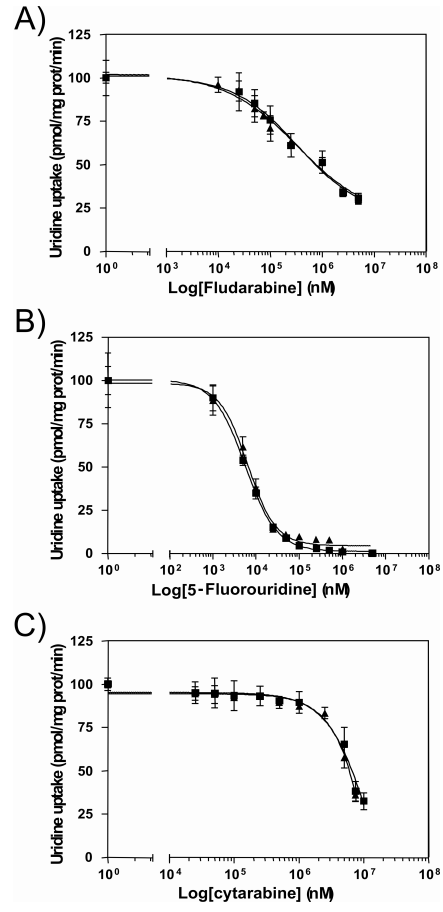


Figure 6

